

# **DEVELOPING A PORTABLE BLOOD GLUCOSE METER USING RAMAN SPECTROSCOPY TECHNIQUE**

by

Akraradet Sinsamersuk

A Dissertation Submitted in Partial Fulfillment of the Requirements for the Degree of  
Doctor of Engineering in Data Science and Artificial Intelligence

Examination Committee: Dr. Chaklam Silpasuwanchai (Chairperson)  
Dr. Chutiporn Anutariya  
Dr. Attaphongse Taparugssanagorn  
Dr. Raffaele Ricco

Nationality: Thai

Previous Degree: Master of Engineering in Computer Science  
Asian Institute of Technology  
Pathum Thani, Thailand

Scholarship Donor: Royal Thai Government

Asian Institute of Technology  
School of Engineering and Technology  
Thailand  
August 2022

## ABSTRACT

Self-monitoring of blood glucose (SMBG) is essential for diabetics to monitor their glycemia (the concentration of sugar or glucose in the blood). By measuring glycemia continuously, the treatment and patient lifestyle can be adjusted according to the report. The solution would be a wearable device that collects blood glucose continuously throughout the day. However, building a complete non-invasive one is challenging. Multiple techniques employing non-optical and optical methods have been studied. One technique that showing to be promising for this task is Raman Spectroscopy due to its low sensitivity to water and temperature, and great specificity. Fortunately, researchers have shown that glycemia can be measured by observing the light scattering such as the Raman Spectroscopy technique. With this method, it is possible to develop portable blood glucose meter equipment that is not only non-invasive but also a continuous method. Our portable equipment has an accuracy comparable to the clinical glucose meter of choice with an error of less than  $\pm 0.83$  mmol/L. The portable aspect enables continuous sampling throughout the day. With our equipment, continuous non-invasive SMBG is possible. Not only this will help to improve the treatment plan for diabetics but also enables individuals to monitor their glycemia which in turn may improve their diet selection.

# CONTENTS

	Page
<b>ABSTRACT</b>	<b>ii</b>
<b>LIST OF TABLES</b>	<b>iv</b>
<b>LIST OF FIGURES</b>	<b>v</b>
<b>CHAPTER 1 INTRODUCTION</b>	<b>1</b>
1.1 Background of the Study	1
1.2 Statement of the Problem	1
1.3 Objectives	2
1.3.1 Study 1: Confirming the parameters	2
1.3.2 Study 2: Raman scattering of blood glucose study	3
1.3.3 Study 3: Designing and developing wearable blood glucose device	3
1.3.4 Study 4: Device Evaluation	3
1.4 Organization of the Study	3
<b>CHAPTER 2 LITERATURE REVIEW</b>	<b>4</b>
2.1 Measuring Glucose in blood	4
2.2 Glucose fingerprint	4
2.3 Relationship of Raman scattering and glucose concentration	6
2.4 Concentration Limitation	8
<b>CHAPTER 3 METHODOLOGY</b>	<b>9</b>
3.1 Study 1: Confirming the parameters	9
3.2 Study 2: Raman scattering of blood glucose study	9
3.3 Study 3: Designing and developing wearable blood glucose device	9
3.4 Study 4: Device Evaluation	9
<b>REFERENCES</b>	<b>10</b>

## LIST OF TABLES

Tables	Page
Table 2.1 Assignments of Raman peaks that are identified in the spectra of the microvessels and blood (Chaiken et al., 2001; Enejder et al., 2005; Lemler, Premasiri, DelMonaco, & Ziegler, 2014; Magnussen et al., 2017)	7

## LIST OF FIGURES

Figures	Page
Figure 2.1 Raman spectra of (A) galactose and (B) glucose, both crystalline. $\lambda_{ex}$ 532 nm, $P$ 20 mW, $t_{ac}$ 2 min (Lyandres et al., 2008)	5
Figure 2.2 Raman spectra of glucose solution at different concentration (Shao et al., 2012).	5
Figure 2.3 Raman spectra of lyophilized glucose compare with blood glucose measure at wrist (González Viveros et al., 2022).	5
Figure 2.4 (A) Raman spectra of blood glucose obtained by subtracting two Raman signals (Kang et al., 2020).	6
Figure 2.5 (A) Raman spectra of blood glucose measure at nailfold (Li et al., 2019).	6
Figure 2.6 (A) Blood glucose value with $1125\text{ cm}^{-1}$ relative intensity. (B) Concentration-dependent Raman relative intensities of glucose ( $1125\text{ cm}^{-1}$ ) (Shao et al., 2012)	8

# CHAPTER 1

## INTRODUCTION

### 1.1 Background of the Study

Building a wearable blood glucose device can help diabetes to monitor their glycemic throughout the day. The term "wearable" could be seen as a combination of non-invasive, continuous, and portable devices. Currently, continuous glucose monitoring (CGM) systems have been recognized as the ideal monitoring systems for glycemic control of diabetic patients (Lee, Probst, Klonoff, & Sode, 2021). However, current CGM devices are not reliable in terms of accuracy and required sensor implantation which considers being a minimally invasive (Keenan, Mastrototaro, Voskanyan, & Steil, 2009)

Fortunately, the analyte analysis noninvasive techniques have been studied as a means to measure glycemic continuously. Among techniques, the ones using optical methods yield a better result (Sim, Ahn, Jeong, & Kim, 2018). Ranging from far infrared to fluorescence spectroscopy, Raman spectroscopy is the most interesting technique. Not only it is insensitive to water, but it is also shown to be able to quantitatively measure glucose transcutaneously (Kang et al., 2020). Recently, *Quantum Operation Inc.* (2022) shows the prototype of a wearable blood glucose smartwatch that employs Raman spectroscopy. However, evidence of a workable device is absent.

### 1.2 Statement of the Problem

One important variable that impact the overall design of the wearable device is the measuring site. Forearm (Enejder et al., 2005; Scholtes-Timmerman, Bijlsma, Fokkert, Slingerland, & Veen, 2014), thenar (Lundsgaard-Nielsen et al., 2018), and nail fold (Li et al., 2019) have been selected as measuring sites with promising results. While González Viveros et al. (2022) shows that the forearm is the most effective site compared to the wrist and index finger, it remains unclear which site is the best due to different equipment, parameters, methodology, and analysis styles across the papers.

The experiment must be conducted to finalize and confirm the measuring scheme. Raman spectroscopy with 785 nm laser was used in (González Viveros et al., 2022; Li et al., 2019; Scholtes-Timmerman et al., 2014) and showed success. However, the schemes were different. Measuring configuration is 10 times accumulation of 10 seconds expo-

sure in Scholtes-Timmerman et al. (2014), nine times accumulation of 30 seconds exposure in (González Viveros et al., 2022), and six times accumulation of 40 seconds exposure in (Li et al., 2019). Since we want to develop a wearable device, a benchmark of 15 seconds is chosen following the SpO2 measuring of the Apple Watch 8 (*Measure blood oxygen levels on Apple Watch*, 2022).

Data were obtained using the oral glucose tolerance test (OGTT) from 12 volunteers for 10 days in (Li et al., 2019), a single collection from 46 volunteers (including 32 type-2 diabetes, 10 prediabetes) in (González Viveros et al., 2022) and from 166 patients in (Scholtes-Timmerman et al., 2014). All labels were obtained by drawing a blood sample from the subject.

Modeling the data with multiple linear regression (MLR) + hand-pick features (911, 1060, 1125, 1450  $\text{cm}^{-1}$ ) result in prediction correlation  $R = 0.85$  for intrasubject cross-validation (CV) and  $R = 0.91$  for intersubject CV (Kang et al., 2020), a back propagation artificial neural network (BP-ANN) + principal component analysis (PCA) achieved root-means-square error (RMSE) of 0.45 mmol/L and  $R^2$  of 0.95 for intrasubject modeling and RMSE of 0.27 and  $R^2$  of 0.98 for intersubject modeling (Li et al., 2019). González Viveros et al. (2022) showed the use of self-organizing maps (SOM) + RReliefF as automatic feature selection and feed-forward artificial neural networks (FFNN) can achieve up to RMSE of 30.12 mg/dL (1.7 mmol/L).

### 1.3 Objectives

Our objective is to develop a wearable self-monitoring blood glucose meter. To achieve this, we separate the project into two studies.

#### 1.3.1 Study 1: Confirming the parameters

The first study aims to confirm the parameters starting from laser selection (wavelength), measuring time, and measuring site. For now, we pre-select the laser to 785 nm as it offers (1) good skin penetration the skin compared to 830 nm (Sim et al., 2018), (2) availability of cost-efficient and compact, high-quality laser sources (Photonics, 2021). The measuring time has to be tested with the actual Raman Instrument. The measuring site will be the index fingertip, index nail fold, wrist, and forearm.

Metric: A fingerprint of glucose should be presented (high correlation) with minimal

fluorescence and total time.

Outcome: Ranking measuring sites by correlation. Confirm measuring time.

### ***1.3.2 Study 2: Raman scattering of blood glucose study***

The second study aims to understand and reproduce the Raman scattering of blood glucose. This study will require 15 subjects for data collection using the OGTT scheme. The preprocessing and modeling will be done following the previous works. At this stage, the performance and power consumption of models will be recorded for the next study.

Metric: Selected features are agreed to in prior works. Modeling achieves over 80% of Clarke error grid (CEG) zone A.

Outcome: By performing  $\Delta G$  (Kang et al., 2020), we confirm the peak of glucose in the blood. Confirm the model to use.

### ***1.3.3 Study 3: Designing and developing wearable blood glucose device***

The third study aims to finalize the design of our wearable device and develop a prototype. The feature will include storage for self-data collection and upload to the cloud.

Metric: Workable device with blood glucose prediction similar to the 1.3.2.

Outcome: Prototype device.

### ***1.3.4 Study 4: Device Evaluation***

The fourth study aims to evaluate the prototype. We repeat the 1.3.2 experiment but this time substituting Raman instrument with our prototype.

Metric: CEG zone A.

Outcome: The prototype achieve over 80% of CEG zone A.

## **1.4 Organization of the Study**

Start your paragraph here.



## CHAPTER 2

### LITERATURE REVIEW

Write your introductory paragraph/s to give an overview of the chapter (except for Chapter 1). Limit this section to two paragraphs. Follow the appropriate structure of writing paragraphs. Paragraphs should have at least four sentences (8 lines). Paragraphs with more than 6 sentences (12 lines) must be split into two paragraphs. Maintain one blank line between paragraphs.

#### 2.1 Measuring Glucose in blood

Measured Raman signal can be seen as four parts Kang et al. (2020). (1) glucose Raman spectrum ( $G$ ), (2) tissue (non-glucose) Raman spectrum ( $T$ ), (3) time-varying tissue background signal ( $B_T$ ), and (4) time-independent system background signal ( $B_S$ ). Glucose signals changes according to the amount of glucose that exists in the blood. This means  $\Delta G = G_{t_1} - G_{t_2}$  where  $G_{t_1}$  and  $G_{t_2}$  is glucose signal at time  $t_1$  and  $t_2$  respectively. Tissue Raman is generated by lipids, proteins, and collagen. When measuring the same spot, the tissue Raman stays relatively unchanged. This means  $\Delta T = T_{t_1} - T_{t_2} \approx 0$ . For time-varying tissue background and time-independent system background, the difference at two-time points is  $\Delta B_T = B_{T_{t_1}} - B_{T_{t_2}}$  and  $\Delta B_S = B_{S_{t_1}} - B_{S_{t_2}}$ . Given the  $\Delta t$  is small,  $\Delta B_T$  and  $\Delta B_S$  is  $\approx 0$ .

The Raman signal ( $R$ ) consists of four parts that can be modeled as  $R = G + T + B_T + B_S$ . Then, the  $\Delta R$  would be  $\Delta G + \Delta T + \Delta B_T + \Delta B_S$ . It is obvious that, given  $\Delta t$  is small, the  $\Delta R = \Delta G + 0 + 0 + 0 = G_{t_1} - G_{t_2}$ .

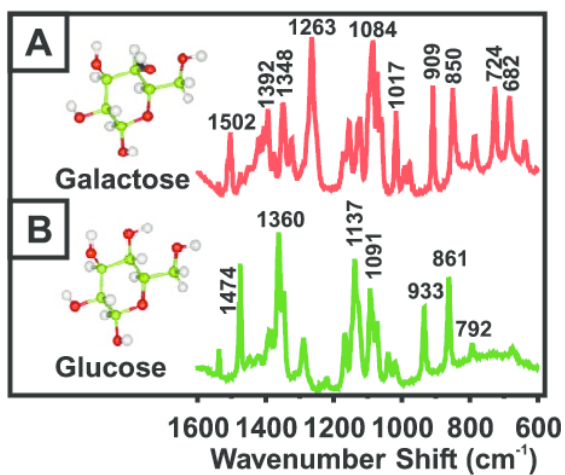
#### 2.2 Glucose fingerprint

Figure 2.1 shows the direct measurement Raman scattering of crystalline glucose using 20 mW 532 nm laser (Lyandres et al., 2008). The numbers indicate in the figure are the signature peaks of glucose in crystalline form. The number are 792, 861, 933, 1091, 1137, 1360, and 1474  $\text{cm}^{-1}$ .

Figure 2.2 shows the Raman shift of glucose solution at different concentrations. Here, the peaks are 796, 1060, 1142, and 1366  $\text{cm}^{-1}$ . Comparing the peaks of the two glucose form, the wavenumber of peaks are close but the height is not.

**Figure 2.1**

Raman spectra of (A) galactose and (B) glucose, both crystalline.  $\lambda_{ex}$  532 nm,  $P$  20 mW,  $t_{ac}$  2 min (Lyandres et al., 2008)



**Figure 2.2**

Raman spectra of glucose solution at different concentration (Shao et al., 2012).

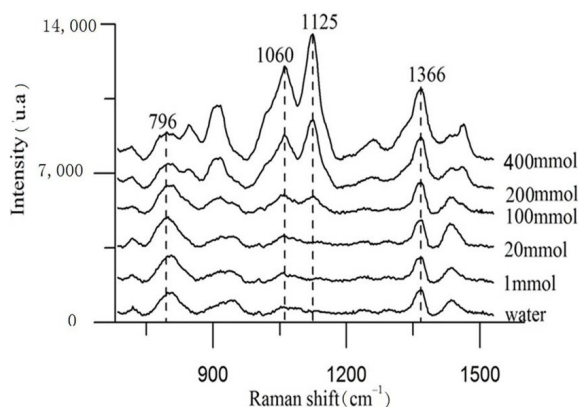


**Figure 2.3**

Raman spectra of lyophilized glucose compare with blood glucose measure at wrist (González Viveros et al., 2022).

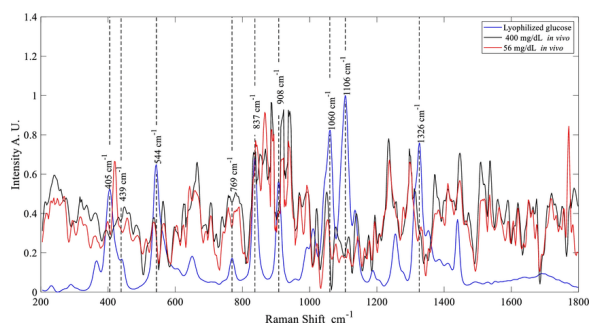


**Figure 2.4**

(A) Raman spectra of blood glucose obtained by subtracting two Raman signals (Kang et al., 2020).

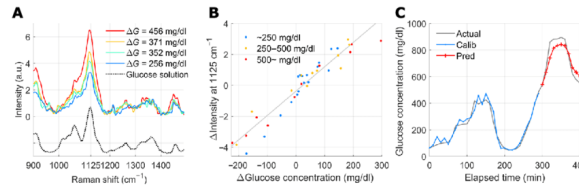
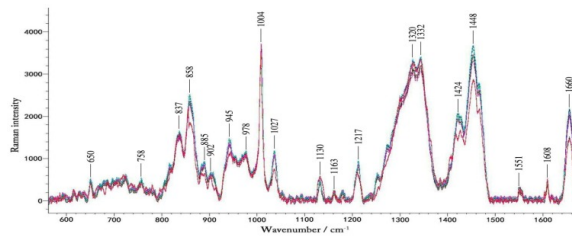


**Figure 2.5**

(A) Raman spectra of blood glucose measure at nailfold (Li et al., 2019).



González Viveros et al. (2022) reported the peaks of lyophilized (Freeze-drying) glucose and compared with blood glucose measured from the wrist (Figure 2.3). The reported peaks of lyophilized glucose are 405, 439, 544, 769, 837, 908, 1060, 1106, and 1326  $\text{cm}^{-1}$ . For the forearm peaks at 544, 837, and 1060  $\text{cm}^{-1}$ . For the wrist, the peaks at 544 and 837  $\text{cm}^{-1}$ . And, the index finger at 544 and 837  $\text{cm}^{-1}$ . Molecular vibrations per each peak are 544  $\text{cm}^{-1}$  exocyclic deformation (Ilaslan, Boyaci, & Topcu, 2015), 837  $\text{cm}^{-1}$  vibrations  $\nu(\text{C}-\text{C})$  (Owora, 2018), and 1060  $\text{cm}^{-1}$  stretching  $\nu(\text{C}-\text{O})$  and  $\nu(\text{C}-\text{C})$  (Ilaslan et al., 2015; Özbalci, Boyaci, Topcu, Kadilar, & Tamer, 2013).

For measuring glucose in the blood, Kang et al. (2020) showed the Raman shift obtained by subtracting the two Raman signals showed a significant peak at 1125  $\text{cm}^{-1}$  (Figure 2.4A). Figure 2.5 shows the peaks number that agreed with the other works (837, 858, 945, 1027, 1130, and 1448  $\text{cm}^{-1}$ ). In addition, Table 2.1 shows what to expect when the Raman signal is measured correctly.

### 2.3 Relationship of Raman scattering and glucose concentration

In glucose solution, the concentration of 0.1 - 40 mmol/L of glucose in water and Raman shift at 1125  $\text{cm}^{-1}$  has a linear relationship Shao et al. (2012). The same case can not be said with blood glucose. Since blood contains multiple components, using 1125  $\text{cm}^{-1}$  directly will not work. Kang et al. (2020) shows that the ratio of 1125 and 1450 (pro-

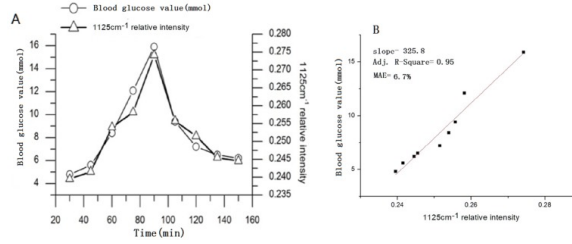
**Table 2.1**

*Assignments of Raman peaks that are identified in the spectra of the microvessels and blood (Chaiken et al., 2001; Enejder et al., 2005; Lemler et al., 2014; Magnussen et al., 2017)*

Peak Position (cm <sup>-1</sup> )		Assignments	Components
Microvessels	Blood		
650	643	P:C-S str	Ascorbic acid
758	752	$\nu_{15}$	Trp
837	827	$\gamma_{10}$	Fructose
858	855	$\nu(C - C)$	Tyr, lac
885	-	-	-
902	898	p:C-C skeletal	Tyr
945	940	$\nu(C - C)$	Crtic acid
978	971	p: Skeletal vibr	Fibrin
1004	1004	$\nu$ -ring	Phe
1027	1026	$\delta(= C_b H_2)$ asym	Lac
1130	1129	$\nu_5$ ,	Lac
1163	1157	$\nu_{44}$	Heme
1217	1212	$\nu_5 + \nu_{18}$	Heme
1320	1321	p: CH <sub>2</sub> twist	Try
1332	1341	$\nu_{41}$	Trp
1424	1423	$\nu_{28}$	Acetates
1448	1450	$\delta(= CH_2/CH_3)$	Trp
1551	1546	$\nu_{11}$	Heme
1608	1603	$\nu(C = C)_{\text{venyl}}$	Heme
1660	1653	Amide I	Heme

**Figure 2.6**

(A) Blood glucose value with  $1125\text{ cm}^{-1}$  relative intensity. (B) Concentration-dependent Raman relative intensities of glucose ( $1125\text{ cm}^{-1}$ ) (Shao et al., 2012)



tein/lipid peak)  $\text{cm}^{-1}$  yield a linear relationship. Figure 2.6 shows that the normalized  $1125\text{ cm}^{-1}$  has a linear relationship with the glucose concentration. This same procedure is also presented in (Shao et al., 2012) where  $1549\text{ cm}^{-1}$  is used to normalize the spectrum. On the other hand, Li et al. (2019) uses PCA and BP-ANN with an input layer of 3, a hidden layer of 4, and an output layer of 1. While the model achieved an RMSE of 0.27 in intersubject modeling, using PCA is not necessarily means the features in use is a glucose-related feature (Kang et al., 2020). Adding to the neural network, FFNN is primarily used in modeling glucose in (González Viveros et al., 2022). Without any feature selection, the RMSE of glucose prediction is 3.1 mmol/L and 30.12 mmol after implementing SOM and RReliefF as automatic feature selection.

## 2.4 Concentration Limitation

The usual blood glucose range of a healthy person can be as low as 0.3 - 1 mmol/L and  $<3\text{ mmol/L}$  for diabetics (Shao et al., 2012).

## **CHAPTER 3**

### **METHODOLOGY**

#### **3.1 Study 1: Confirming the parameters**

Kang et al. (2020)

#### **3.2 Study 2: Raman scattering of blood glucose study**

#### **3.3 Study 3: Designing and developing wearable blood glucose device**

#### **3.4 Study 4: Device Evaluation**

## REFERENCES

- Chaiken, J., Finney, W. F., Knudson, P. E., Peterson, K. P., Peterson, C. M., Yang, X., & Weinstock, R. S. (2001). Noninvasive blood analysis by tissue-modulated nir raman spectroscopy. In *Visualization of temporal and spatial data for civilian and defense applications* (Vol. 4368, pp. 134–145).
- Enejder, A. M., Scecina, T. G., Oh, J., Hunter, M., Shih, W., Sasic, S., ... Feld, M. S. (2005). Raman spectroscopy for noninvasive glucose measurements. *Journal of biomedical optics*, 10(3), 031114.
- González Viveros, N., Castro-Ramos, J., Gomez-Gil, P., Cerecedo-Núñez, H., Gutierrez-Delgado, F., Torres Rasgado, E., ... Flores-Guerrero, J. (2022, 09). Quantification of glycated hemoglobin and glucose in vivo using raman spectroscopy and artificial neural networks. *Lasers in Medical Science*, 1-13. doi: 10.1007/s10103-022-03633-w
- Ilaslan, K., Boyaci, I. H., & Topcu, A. (2015). Rapid analysis of glucose, fructose and sucrose contents of commercial soft drinks using raman spectroscopy. *Food Control*, 48, 56–61.
- Kang, J. W., Park, Y. S., Chang, H., Lee, W., Singh, S. P., Choi, W., ... others (2020). Direct observation of glucose fingerprint using in vivo raman spectroscopy. *Science Advances*, 6(4), eaay5206.
- Keenan, D. B., Mastrototaro, J. J., Voskanyan, G., & Steil, G. M. (2009). Delays in minimally invasive continuous glucose monitoring devices: A review of current technology. *Journal of Diabetes Science and Technology*, 3(5), 1207-1214. Retrieved from <https://doi.org/10.1177/193229680900300528> (PMID: 20144438) doi: 10.1177/193229680900300528
- Lee, I., Probst, D., Klonoff, D., & Sode, K. (2021). Continuous glucose monitoring systems - current status and future perspectives of the flagship technologies in biosensor research -. *Biosensors and Bioelectronics*, 181, 113054. Retrieved from <https://www.sciencedirect.com/science/article/pii/S0956566321000919> doi: <https://doi.org/10.1016/j.bios.2021.113054>
- Lemler, P., Premasiri, W., DelMonaco, A., & Ziegler, L. (2014). Nir raman spectra of whole human blood: effects of laser-induced and in vitro hemoglobin denaturation. *Analytical and bioanalytical chemistry*, 406(1), 193–200.
- Li, N., Zang, H., Sun, H., Jiao, X., Wang, K., Liu, T., & Meng, Y. (2019, 04). A nonin-

- vasive accurate measurement of blood glucose levels with raman spectroscopy of blood in microvessels. *Molecules*, 24, 1500. doi: 10.3390/molecules24081500
- Lundsgaard-Nielsen, S., Pors, A., Banke, S., Henriksen, J., Hepp, D., & Weber, A. (2018, 05). Critical-depth raman spectroscopy enables home-use non-invasive glucose monitoring. *PLOS ONE*, 13, e0197134. doi: 10.1371/journal.pone.0197134
- Lyandres, O., Yuen, J. M., Shah, N. C., VanDuyne, R. P., Walsh Jr, J. T., & Glucksberg, M. R. (2008). Progress toward an in vivo surface-enhanced raman spectroscopy glucose sensor. *Diabetes technology & therapeutics*, 10(4), 257–265.
- Magnussen, L., Hvid, L., Hermann, A., Hougaard, D., Gram, B., Caserotti, P., & Andersen, M. (2017). Testosterone therapy preserves muscle strength and power in aging men with type 2 diabetes—a randomized controlled trial. *Andrology*, 5(5), 946–953.
- Measure blood oxygen levels on Apple Watch.* (2022). <https://support.apple.com/guide/watch/blood-oxygen-apdaf17aa5ef/watchos>. ([Online; accessed 2022-11-09])
- Owora, A. H. (2018). Diagnostic validity and clinical utility of hba1c tests for type 2 diabetes mellitus. *Current diabetes reviews*, 14(2), 196.
- Özbalci, B., Boyaci, İ. H., Topcu, A., Kadılar, C., & Tamer, U. (2013). Rapid analysis of sugars in honey by processing raman spectrum using chemometric methods and artificial neural networks. *Food chemistry*, 136(3-4), 1444–1452.
- Photonics, H. (2021, may 10). *Which 785 nm laser for raman spectroscopy?* <https://hubner-photonics.com/knowledge-bank/which-785-nm-laser-for-raman-spectroscopy/>. ([Online; accessed 2022-11-09])
- Quantum operation inc.* (2022). <https://quantum-op.co.jp/en>. (Online; accessed 2022-11-09)
- Scholtes-Timmerman, M., Bijlsma, S., Fokkert, M., Slingerland, R., & Veen, S. (2014, 07). Raman spectroscopy as a promising tool for noninvasive point-of-care glucose monitoring. *Journal of diabetes science and technology*, 8. doi: 10.1177/1932296814543104
- Shao, J., Lin, M., Li, Y., Li, X., Liu, J., Liang, J., & Yao, H. (2012). In vivo blood glucose quantification using raman spectroscopy. *PloS one*, 7(10), e48127.
- Sim, J., Ahn, C.-G., Jeong, E.-J., & Kim, B. (2018, 01). In vivo microscopic pho-



toacoustic spectroscopy for non-invasive glucose monitoring invulnerable to skin secretion products. *Scientific Reports*, 8. doi: 10.1038/s41598-018-19340-y